Multifunctional essentiality of succinate metabolism in adaptation to hypoxia in *Mycobacterium tuberculosis*

Hyungjin Eoh and Kyu Y. Rhee[1]

Division of Infectious Diseases, Department of Medicine, Weill Cornell Medical College, New York, NY 10065

Edited by Vern L. Schramm, Albert Einstein College of Medicine of Yeshiva University, Bronx, NY, and approved March 8, 2013 (received for review November 7, 2012)

Mycobacterium tuberculosis **is a chronic, facultative intracellular pathogen that spends the majority of its decades-long life cycle in a non- or slowly replicating state. However, the bacterium remains poised to resume replicating so that it can transmit itself to a new host. Knowledge of the metabolic adaptations used to facilitate entry into and exit from nonreplicative states remains incomplete. Here, we apply ^{13}C-based metabolomic profiling to characterize the activity of *M. tuberculosis* tricarboxylic acid cycle during adaptation to and recovery from hypoxia, a physiologically relevant condition associated with nonreplication. We show that, as *M. tuberculosis* adapts to hypoxia, it slows and remodels its tricarboxylic acid cycle to increase production of succinate, which is used to flexibly sustain membrane potential, ATP synthesis, and anaplerosis, in response to varying degrees of O_2 limitation and the presence or absence of the alternate electron acceptor nitrate. This remodeling is mediated by the bifunctional enzyme isocitrate lyase acting in a noncanonical role distinct from fatty acid catabolism. Isocitrate lyase-dependent production of succinate affords *M. tuberculosis* with a unique and bioenergetically efficient metabolic means of entry into and exit from hypoxia-induced quiescence.**

Quiescence, or exit from cell cycle, is a physiologic prerogative of all cells, executed irreversibly by some upon terminal differentiation and reversibly by others as they adapt to changing conditions (1). For *Mycobacterium tuberculosis*, the causative agent of tuberculosis (TB), quiescence has emerged as a hallmark of its pathogenicity. *M. tuberculosis* infects approximately one in every three people worldwide and is the leading bacterial cause of death. Following infection, *M. tuberculosis* enters a clinically asymptomatic state of non- or slowly replicating physiology that often lasts decades, if not the lifetime, of the infected host, and exhibits a form of nonheritable resistance to nearly all TB drugs that has hindered mass eradication strategies (2). Clinical TB arises when *M. tuberculosis* reenters cell cycle and provokes an inflammatory response that inflicts host tissue damage and enables it to transmit itself to a new host. However, some of the *M. tuberculosis* in active TB is nonreplicating. This is thought to impose the need for chemotherapies that are longer and more complex than for virtually any other bacterial infection (2–7). However, biochemical knowledge of quiescent *M. tuberculosis* remains highly incomplete.

Relieved of the requirement to double biomass, quiescent cells have generally been perceived to have minimal metabolic activity. However, quiescent cells often occupy ecological niches that are highly dynamic and face the challenge of preserving both their viability and their ability to reenter cell cycle. Fibroblasts induced into quiescence by contact inhibition metabolized glucose through all branches of central carbon metabolism at a rate similar to those of proliferating cells (8). Such studies have suggested that quiescence may be associated with a redirection, rather than bulk reduction, of metabolic activity.

During its decades-long life cycle, *M. tuberculosis* encounters diverse host-imposed stringencies, such as those associated with residence within macrophages in granulomas (3, 4, 7, 9, 10). Each known host-imposed stringency is capable of inducing *M. tuberculosis* to exit its cell cycle. Among these, hypoxia has long been considered a feature faced by *M. tuberculosis* in humans and in some experimental animal models (11–15). *M. tuberculosis* exposed to hypoxia in vitro has been shown to cease replication but some proportion remain viable and virulent for decades, tolerant to nearly all first and second line TB drugs (16, 17).

Hypoxic *M. tuberculosis* down-regulates transcription of key complexes of the electron transport chain (ETC) and maintains ATP levels approximately five times lower than those of replicating counterparts (18, 19). However, even under hypoxic conditions, sustained production of ATP, regeneration of NAD, and maintenance of proton motive force are required to preserve viability. Previous work identified a genetic regulon (DosR) essential for mediating adaptation to O_2 limited environments and during reversible shifts between aerobic and anaerobic respiration (13, 20–23). However, the metabolic changes accompanying *M. tuberculosis* exit and entry into cell cycle remain incompletely defined.

Here, we applied liquid chromatography–time-of-flight mass spectrometry to monitor the pool size and turnover of metabolites in *M. tuberculosis* during its transitions through hypoxia-induced quiescence, focusing on intermediates of its putative tricarboxylic acid (TCA) cycle. The TCA cycle consists in a highly conserved set of biochemical reactions that serve to generate ATP, biosynthetic precursors and reducing equivalents. Recent work, using a chemostat model, showed that hypoxic *M. tuberculosis* metabolize glucose through a reverse TCA cycle to generate succinate as an obligatorily secreted fermentation product (24). However, prevailing evidence has implicated fatty acids and lipids as key carbon sources encountered by *M. tuberculosis* in the host, whose metabolism could not be readily supported by the foregoing mechanism (10, 25–28). We therefore sought to expand our understanding of the scope and nature of metabolic adaptations used by *M. tuberculosis* to enter into, reside in, and exit from hypoxia-induced quiescence.

Results

Replicative Quiescence of *M. tuberculosis* at 1% O_2. We adapted our previously described filter culture method to model hypoxia-regulated entry and exit of *M. tuberculosis* into and out of cell cycle by combining a chemically defined agar medium with a disposable environmental chamber that depletes oxygen gradually and generates CO_2 via a palladium catalyst (29, 30). This system achieves a final atmosphere of ~1% O_2 (as reported by a resazurin-based indicator strip) and ~5% CO_2, levels similar to those encountered in the tuberculous lungs of infected animals, within 4 h (31–33). We chose acetate as a carbon source based on genetic evidence implicating fatty acids as a potential carbon source encountered by

Author contributions: H.E. and K.Y.R. designed research; H.E. performed research; H.E. and K.Y.R. analyzed data; and H.E. and K.Y.R. wrote the paper.

The authors declare no conflict of interest.

This article is a PNAS Direct Submission.

[1]To whom correspondence should be addressed. E-mail: kyr9001@med.cornell.edu.

This article contains supporting information online at www.pnas.org/lookup/suppl/doi:10.1073/pnas.1219375110/-/DCSupplemental.

M. tuberculosis during both the acute and chronic phases of infection (25–27, 34, 35). Using this system, we confirmed that *M. tuberculosis* neither underwent net replication nor death in response to incubation at 1% O_2 and resumed growth upon reaeration (Fig. S1 *A* and *B*). We further showed that this system was associated with both the reversible biphasic induction of *dosR*, a previously validated transcriptional marker of hypoxia, and accompanying reductions of levels of ATP and NAD (Fig. S1 *C–F*) (18, 23, 36). Based on this validation, we proceeded to monitor TCA cycle activity in response to, during, and after O_2 depletion by either transferring cells from unlabeled to uniformly ^{13}C labeled ([U-^{13}C]) acetate at the time of exposure to hypoxia and/or reaeration or by pulsing with [U-^{13}C] acetate-containing medium once *M. tuberculosis* had adapted and sampling at serial time points thereafter.

Metabolic Slowing and Remodeling of TCA Cycle Activity in *M. tuberculosis* at 1% O_2. In response to hypoxia, *M. tuberculosis* decreased nutrient uptake and/or consumption by 80%, as reported by residual [U-^{13}C] acetate levels in the medium (Fig. S2*A*). This decrease was accompanied by a slowdown in TCA cycle activity, as reported by the ^{13}C-labeling patterns of its intermediates (Fig. S2 *B–D*), and reached a metabolic steady state after 12–24 h. In addition, all changes could be restored with reaeration (Fig. S3 *A* and *B*). Canonical TCA cycle activity results in the progressive assimilation of acetate-based C_2 units, manifest by the accumulation of higher order $^{13}C_2$-based isotopologues when cells are grown in [U-^{13}C] acetate-containing medium. The coordinate downshift of dominant ^{13}C-labeled isotopologues for all TCA cycle intermediates from +6 (or +4) to +2 ^{13}C-labeled forms (Fig. S4 *A* and *B*) thus revealed hypoxia-induced slowing of TCA cycle activity. Consistent with this slowing, we observed an accompanying decrease in gluconeogenic carbon flow, reported by a near complete loss of ^{13}C-labeling of pyruvate (Fig. 1 and Figs. S3*B* and S4*B*). ^{13}C-labeling analysis of TCA cycle activity of quiescent *M. tuberculosis* (preadapted to 1% O_2) confirmed a sustained downshift of $^{13}C_2$-labeled isotopologues for TCA cycle intermediates compared with those from aerobic controls (Fig. S4 *A* and *B*).

In addition to the broad quantitative decrease in TCA cycle activity described above, we discovered a more complex pattern of changes in the levels and labeling patterns of specific TCA cycle intermediates. In response to O_2 depletion, the level of α-ketoglutarate decreased threefold, whereas levels of succinate, malate, and aspartate (a surrogate of oxaloacetate) increased 6.5-, 1.4-, and 1.8-fold, respectively (Fig. 1). This pattern was indicative of an activation of *M. tuberculosis* isocitrate lyases (ICLs), which serve dual roles in the glyoxylate shunt and methylcitrate cycles, and have previously been reported to be up-regulated in *M. tuberculosis* in response to hypoxia and essential for survival of bacillus Calmette–Guérin at low growth rates (37, 38). Accordingly, we observed a hypoxia-induced increase in *icl* transcript levels even when *M. tuberculosis* was already metabolizing acetate (Fig. 2*A*) (15, 26, 39). However, the disproportionately large accumulation of succinate in comparison with malate or aspartate was not consistent with a simple switch to a glyoxylate shunt-based TCA cycle. Moreover, the isotopic labeling pattern of this accumulated succinate predominantly contained two, rather than four, ^{13}C atoms, as was also the case for malate and aspartate (Fig. S4 *A* and *B*). This is indicative of both a slowdown of TCA cycle activity, rather than a switch to a glyoxylate shunt-based TCA cycle, as well as potential increase in methylcitrate cycle activity, as evidenced by the disproportionately large increase in ^{13}C labeling of succinate over citrate/isocitrate (Fig. 1). In addition, the accumulation of succinate was not associated with proportional increases in the production of malate or aspartate from extracellular ^{13}C acetate (as would be revealed by an increase in the level of labeled malate and aspartate) or from turnover of preexisting macromolecules or other metabolic stores, as would

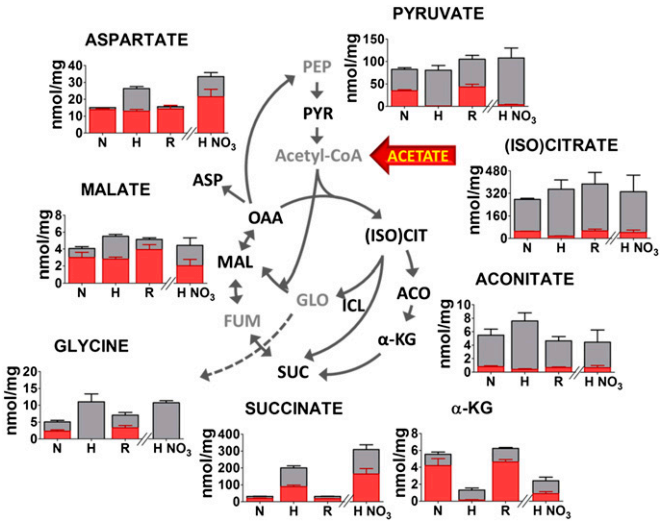

Fig. 1. Hypoxia-associated remodeling of *M. tuberculosis* TCA cycle activity. Intrabacterial pool sizes and isotopic labeling of TCA cycle-related intermediates in *M. tuberculosis* incubated in [U-^{13}C]acetate-containing media for 24 h at 21% O_2 (N), 1% O_2 (H), and at 21% O_2 following preincubation at 1% O_2 for 48 h (R). Intrabacterial pool sizes and isotopic labeling of the intermediates in *M. tuberculosis* incubated at 1% O_2 supplemented with 5 mM nitrate (H NO_3) was also included at the end of individual graph. Total bar heights indicate the intrabacterial concentration, whereas the red colored area of each bar denotes the extent of ^{13}C labeling achieved following transfer to [U-^{13}C] acetate-containing media under the condition indicated. All values are average of independent triplicate experiments ±SEM. α-KG, α-ketoglutarate; ACO, aconitate; ASP, aspartate; FUM, fumarate; GLO, glyoxylate; ICL, Isocitrate lyase; (ISO)CIT, (iso)citrate; MAL, malate; PEP, phosphoenolpyruvate; PYR, pyruvate; SUC, succinate.

be revealed by the increase in unlabeled pools of succinate, malate, and aspartate. *M. tuberculosis* adapted to hypoxia also showed twofold higher levels of glycine (Fig. 1), a product previously predicted to arise from glyoxylate via an accompanying increase in glycine dehydrogenase activity (15). Importantly, similar results were also observed when using glucose as a carbon source (Fig. S5). These results thus suggest that *M. tuberculosis* may remodel its TCA cycle in response to hypoxia by activating its glyoxylate shunt to produce succinate and glycine as end products rather than intermediates.

Isocitrate Lyase-Mediated Production of Succinate and Its Role in *M. tuberculosis* Survival at 1% O_2. We tested the specific role of the glyoxylate shunt enzymes isocitrate lyase (*icl1* and *icl2*, collectively referred to as ICL) as a mediator of the foregoing increase in succinate by comparing the metabolic profiles and in vitro survival of wild-type and ICL-deficient *M. tuberculosis* strains. *M. tuberculosis* ICLs are essential for metabolism and growth on fatty acid substrates due to their bifunctional activities as isocitrate and methylisocitrate lyases (26, 27). We obviated this potentially confounding metabolic role by culturing *M. tuberculosis* strains on glucose, a growth permissive carbon source that resulted in the same hypoxia-induced changes in TCA cycle metabolites as described for acetate (Fig. 1 and Fig. S5). As shown in Fig. 2*B*, ICL-deficient *M. tuberculosis* cultured on glucose-containing medium exhibited a 2–3 $\log_{10}$ reduction in colony forming units (CFUs) in response to hypoxia. The decline in CFUs was preceded by specific reductions in levels of succinate, malate, and aspartate (Fig. 2*C*). No such reductions were observed in wild-type *M. tuberculosis* cultured at 1% O_2 or in ICL-deficient *M. tuberculosis* cultured in 21% O_2 (Figs.1 and 2*C*). We further found that this essentiality could be mitigated by aspartic acid, a reductive precursor of succinate (Fig. 2*D* and Fig. S6), thereby confirming the activity of

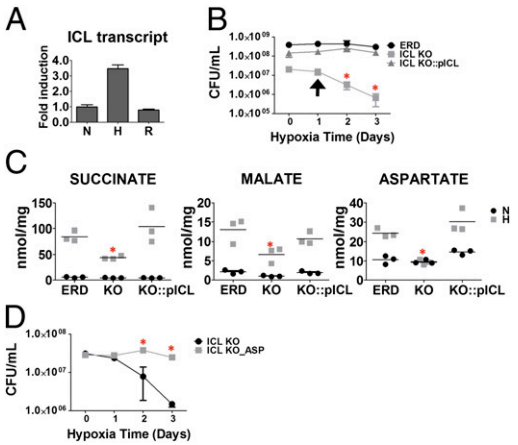

Fig. 2. Genetic essentiality of isocitrate lyase for metabolic adaptation and viability of *M. tuberculosis* to 1% O_2. (*A*) *icl1* transcript levels following incubation for 24 h at 21% O_2 (N), 1% O_2 (H), and at 21% O_2 following reaeration of *M. tuberculosis* preincubated at 1% O_2 for 48 h (R). Transcript levels were analyzed by qRT-PCR, normalized to *sigA* transcript levels, and expressed as fold change relative to that observed at 21% O_2. (*B*) Viability of Erdman wild type (black circles), Δ*icl1/2* knockout (gray squares), and Δ*icl1/2* knockout complemented with *icl1* (dark gray triangles) incubated at 1% O_2 with 0.2% glucose for various time points. Arrow denotes the time point when metabolomic profiles (shown in Fig. 2*C*) were generated. (*C*) Intrabacterial pool sizes of TCA cycle intermediates (succinate, malate, and aspartate) in Erdman wild type (ERD), Δ*icl1/2* knockout (KO), and Δ*icl1/2* knockout complemented with *icl1* (KO::pICL) cultured in media containing 0.2% [U-^{13}C] glucose, a permissive carbon source (27) following incubation for 24 h at either 21% O_2 (black circles) or 1% C_2 (gray squares). (*D*) Viability of Δ*icl1/2* knockout *M. tuberculosis* at 1% O_2 in the presence (black circles) or absence (gray squares) of a precursor of reductive TCA cycle intermediates (30 mM aspartate). $^*P < 0.001$ by ANOVA. All values were the average of at least three experimental replicates in two independent experiments ±SEM.

a reverse TCA cycle and demonstrating that ICL is essential for succinate production in hypoxic conditions. These studies thus established that *M. tuberculosis* ICL is an essential mediator of adaptation to hypoxia because it generates succinate, and possibly glycine, in a manner distinct from its canonical roles in fatty acid metabolism (27).

Succinate-Mediated Maintenance of Membrane Potential in Hypoxic *M. tuberculosis*. Watanabe et al. (24) reported that, lacking an alternate electron acceptor, anaerobically adapted *M. tuberculosis* could metabolize glucose through a reverse TCA cycle to offload unrespired reducing equivalents onto fumarate and generate succinate, whose secretion was proposed to help maintain membrane potential. We sought to understand if the increase in succinate production mediated by ICL, rather than by the reverse TCA cycle, might likewise provide *M. tuberculosis* a means of maintaining membrane potential when metabolizing not only glucose but also acetate in response to O_2 depletion. To address this possibility, we first measured succinate secretion from cells; to this end, we modified our filter culture system by replacing the underlying agar medium with a plastic inset containing chemically equivalent liquid medium in direct contact with the underside of the bacteria-laden filter (Fig. S7*A*). Growth atop this liquid medium was indistinguishable from that achieved on adjacent agar medium and enabled timed start–stop measurements of secretion by sampling the cell-free liquid medium. As shown in Fig. 3*A*, these studies showed a time-dependent accumulation of $^{13}C_2$-labeled succinate in the medium following exposure to and incubation under hypoxic conditions.

Based on these findings, we next tested the impact of inhibiting hypoxia-induced succinate secretion on *M. tuberculosis* viability by adding exogenous succinate to the culture medium as a functional means of inhibiting secretion or efflux of intracellular succinate by concentration-dependent mechanisms (40). We first confirmed that the concentrations of added succinate neither altered the pH of the extracellular medium nor affected *M. tuberculosis* growth under aerobic conditions. We next showed that exogenous succinate impaired secretion of intracellular succinate produced from metabolism of ^{13}C-labeled acetate in hypoxic *M. tuberculosis*, as predicted (Fig. S7*B*). We finally showed that incubation with exogenous succinate selectively impaired both the membrane potential and survival of hypoxic, but not aerated *M. tuberculosis*, as reported by the fluorescent, membrane-permeable dye 3,3′-diethyloxicarbocianide chloride ($DiOC_2$) and CFUs, respectively (Fig. 3 *B* and *C* and Fig. S7*C*) (18, 41). These studies thus establish that succinate secretion is a specific and essential biochemical component of *M. tuberculosis* adaptive response to hypoxia.

Metabolic Essentiality of Succinate Dehydrogenase Activity in Adaptation to Hypoxia. In addition to establishing a role for succinate in sustaining membrane potential, we also evaluated its canonical role as a substrate of succinate dehydrogenase (SDH). SDH couples the oxidation of succinate to the reduction of ubiquinone to ubiquinol and is the only TCA cycle enzyme that is a component of

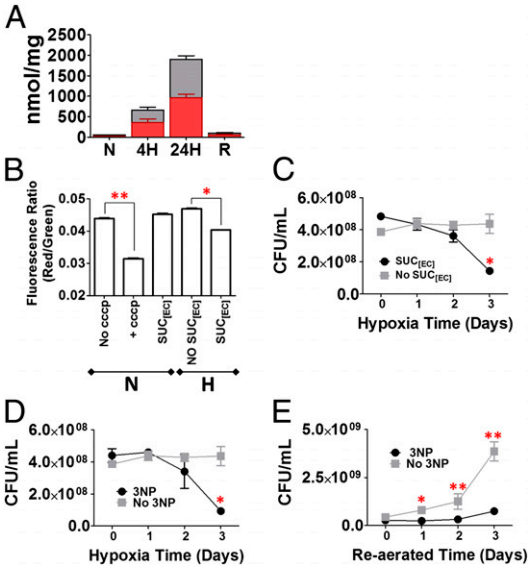

Fig. 3. Multifunctional roles of succinate during adaptation to 1% O_2. (*A*) Time-dependent secretion of succinate following incubation at 21% or 1% O_2 as described (N, 24 h 21% O_2; 4H, 4 h 1% O_2; 24H, 24 h 1% O_2; and R, 24 h reaeration at 21% O_2 following 48 h incubation at 1% O_2). Total bar heights indicate the concentration of secreted succinate; the red colored area of each bar denotes the extent of ^{13}C labeling achieved following transfer to [U-^{13}C] acetate-containing media under the condition indicated. (*B*) Destabilization of *M. tuberculosis* membrane potential following incubation at 1% O_2 in the absence or presence of 2 mM succinate in the extracellular medium. Membrane potential values of *M. tuberculosis* incubated at 21% O_2 (N) or 1% O_2 (H) in the presence ($SUC_{[EC]}$) or absence ($SUC_{[EC]}$) of 2 mM extracellular succinate were compared. Cultures grown under ambient air condition treated with 5 μM of the protonophore carbonyl-cyanide 3-chlorophenylhydrazone (cccp), a membrane depolarization agent, were used as a positive control and those with DMSO (no cccp) were as a vehicle control. (*C*) *M. tuberculosis* viability following incubation at 1% O_2 in the absence or presence of 2 mM succinate in the extracellular medium. (*D* and *E*) *M. tuberculosis* viability following incubation (*D*) in, or reaeration (*E*) from 1% O_2 in the absence or presence of 200 μM 3-nitropropionate (3NP). $^*P < 0.01$ or $^{**}P < 0.001$. All values are the average of experimental triplicates ± SEM and representative of at least two independent experiments.

ETC. We tested the impact of inhibiting *M. tuberculosis* SDH on viability using the suicide inhibitor 3-nitropropionate (3NP) (42). Treatment with 3NP led to an accumulation, rather than a reduction of newly synthesized ^{13}C succinate or accumulation of methycitrate cycle intermediates (Fig. S8 *A* and *B*). This suggested that under the conditions used, the dominant activity of 3NP in intact *M. tuberculosis* was as an inhibitor of SDH, rather than ICL. Although 3NP can inhibit isolated ICL (27), 3NP may act preferentially on SDH in intact *M. tuberculosis* because SDH is located at the membrane rather than in the cytosol. Treatment with 3NP resulted in a time-dependent loss of viability of both wild-type and ΔICL KO *M. tuberculosis* during adaptation to hypoxia that was not observed during reaeration of hypoxic *M. tuberculosis* or in aerobically cultured *M. tuberculosis* (Fig. 3 *D* and *E* and Fig. S8*C*). These findings establish that sustained metabolism of succinate through SDH is an additional essential component of *M. tuberculosis* metabolic adaptation to hypoxia.

Nitrate-Dependent Modulation of TCA Cycle Activity in Hypoxic *M. tuberculosis*. The specific biochemical conditions encountered by *M. tuberculosis* in the host are complex and heterogeneous (3, 4, 7, 9, 10). Nitrate is a natural component of human body fluids that arises in part from dietary sources and in part as a terminal autooxidation product of the nitric oxide produced by the three isoforms of nitric oxide synthase in diverse cells, including immune-activated smooth muscle, epithelial cells, and hematopoietic cells, such as macrophages infected with *M. tuberculosis* (11, 15, 43–45). Both nitric oxide and hypoxia increase *M. tuberculosis* nitrate reductase activity at the whole cell level. Nitrate reduction may enable *M. tuberculosis* to maintain respiratory activity in microaerophilic or hypoxic conditions (44–46). Nitrate is the second most efficient terminal electron acceptor after molecular oxygen and *M. tuberculosis* is the mycobacterial species most capable of using it. In addition, recent work has established the essentiality of nitrate during *M. tuberculosis* adaptation to the rapid onset of anaerobiosis and to acidic, microaerophilic environments (44, 45). We therefore characterized the impact of exogenous nitrate on *M. tuberculosis* TCA cycle activity during adaptation to hypoxia. As shown in Figs. 1 and 4*A* and Fig. S4*B*, provision of nitrate did not alter the pool sizes of most TCA cycle intermediates but did affect their isotopic labeling patterns and reduced the secretion of succinate, leading to larger intracellular pools, as predicted, and relief from the toxic effects of exogenous succinate observed in Fig. 4*B*. Feeding with [U-^{13}C] acetate, for example, led to an upshift in the predominant isotopologue of succinate and malate, from that containing two to that containing four ^{13}C atoms, indicative of an increase in glyoxylate shunt-based TCA cycle activity (Fig. S4*B*). Supplementation of nitrate in culture medium abolished succinate secretion and restored ATP levels, NADH/NAD ratios, and *M. tuberculosis* viability to near aerobic levels (Fig. 4 *A* and *B* and Fig. S1 *G* and *H*). Nitrate thus regulates both the metabolic and respiratory activity of *M. tuberculosis* during adaptation to hypoxia.

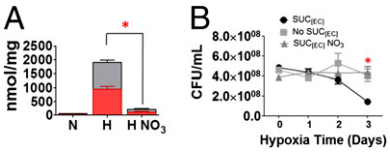

Fig. 4. Nitrate-dependent modulation of TCA cycle activity in hypoxic *M. tuberculosis*. (*A*) Succinate secretion following incubation for 24 h at 21% or 1% O_2 as described (N, 21% O_2; H, 1% O_2; and H NO_3, 1% O_2 supplemented with 5 mM nitrate). Total bar height and red colored area of the bars are as denoted in Figs. 1 and 3*A*. (*B*) *M. tuberculosis* viability following incubation at 1% O_2 in the absence or presence of 2 mM succinate in the extracellular medium as in Fig. 3*C*. *$P < 0.001$ by ANOVA. All values are the average of experimental triplicates ±SEM and representative of at least two independent experiments.

Discussion

Unlike most bacterial pathogens, *M. tuberculosis* spends the majority of its natural life cycle in a state of slowed or arrested replication imposed by humans, its only known natural host. *M. tuberculosis* thus faces the unusual challenge of needing to maintain a metabolic state of replicative quiescence for decades while remaining poised to reenter cell cycle at some point to transmit to a new host and propagate itself as a species (4, 7, 12, 13, 47). However, there has been little knowledge of the metabolic adaptations used by *M. tuberculosis* or other cells to transition in and out of cell cycle.

The present work sheds light on one unique set of such adaptations. Recent work showed that *M. tuberculosis* could operate a reductive TCA half cycle under anaerobic conditions, enabling it to metabolize glucose by generating succinate as an obligatorily secreted, fermentation product of fumarate, following reductive carboxylation of pyruvate or phosphoenolpyruvate to malate and/or oxaloacetate (24). However, evidence has strongly implicated lipids and fatty acids as key carbon sources metabolized by *M. tuberculosis* in the host (10, 25–28). A mechanism functioning only with carbohydrates could not readily accommodate the foregoing carbon sources that include even-chain fatty acids. Our studies thus extend these findings with the discovery of a different metabolic pathway (the glyoxylate shunt) that, in contrast to the above, is capable of supporting metabolism of both glycolytic and fatty acid carbon sources in response to O_2 limitation, yet also produces succinate as its metabolic end product. Moreover, our studies reveal a broader multiplicity of previously unrecognized, essential metabolic roles for succinate during adaptation to O_2 limitation. That is, as O_2 is depleted, *M. tuberculosis* increases expression of the glyoxylate shunt enzyme isocitrate lyase, produces large amount of succinate, and can use this succinate to flexibly sustain membrane potential, ATP synthesis, and anaplerosis, depending on the specific conditions encountered (Fig. S9). Succinate is a bifunctional substrate of SDH, an enzyme that serves both the TCA cycle and ETC and couples carbon flow to ATP synthesis at an efficiency approximately two-thirds that of NADH. Increasing succinate production under O_2 limiting conditions thus enables *M. tuberculosis* to sustain SDH activity and oxidative synthesis of ATP at a rate proportional to its respiratory capacity, while secreting some of the unused excess to maintain membrane potential when an alternative terminal electron acceptor is lacking and/or storing the remainder to enable the immediate resumption of carbon flow and ATP synthesis upon reoxygenation. The near neutral midpoint potential of the succinate/fumarate redox couple ($\varepsilon^{0'}$ = + 0.03 V) makes it suitable to accumulate as a fermentation product of fumarate reductase when metabolizing glycolytic carbon substrates and oxygen is severely limited. Our studies thus reveal that *M. tuberculosis* uses succinate as a type of multifunctional "metabolic battery" capable of flexibly sustaining membrane potential, ATP synthesis, and TCA cycle precursors when O_2 is depleted, while keeping its TCA cycle poised to resume oxidative activity upon access to a terminal electron acceptor, such as nitrate, although the specific mechanisms of nitrate-dependent respiration remain to be elucidated.

Multiple lines of microbiologic, immunohistologic, and biophysical evidence have established hypoxia as a feature of some niches faced by *M. tuberculosis* (3, 13). However, growing evidence has revealed that the extent of hypoxia associated within a given host varies widely based on the size, location, and composition of the microenvironment (31–33). Our studies modeled quiescent *M. tuberculosis* using an O_2 environment of 1%, but the metabolic principle revealed may have broader significance,

namely, the ability of succinate to serve as a biochemical bridge between oxidative and fermentative metabolic states.

Our studies identified a previously unrecognized role for *M. tuberculosis* ICL in adaptation to hypoxia. Enzymatic and transcriptional profiling studies reported that *M. tuberculosis* increased ICL and glycine dehydrogenase activities in response to oxygen limitation, suggesting that *M. tuberculosis* may use ICL to replenish NAD in its oxidized form by offloading NADH-reducing equivalents via a glyoxylate–glycine shunt (15). However, an *M. tuberculosis* strain lacking one of two ICL paralogs was unimpaired in its ability to survive hypoxic or anaerobic incubation (26). Subsequent work showed that a mutant lacking both ICL paralogs was unable to catabolize even- or odd-chain fatty acids (27). Our data now establish that *M. tuberculosis* ICLs (collectively, ICL) are essential for adaptation to hypoxia and that this essentiality is attributable to ICL's ability to supply succinate as a substrate used to sustain hypoxic quiescence, rather than its canonical role in fatty acid catabolism. ICL-deficient *M. tuberculosis* is one of the most severely attenuated mutants tested in a mouse model of TB. Such attenuation may reflect the loss of multiple functions, some of which were revealed by metabolomic studies and could not be foreseen by genetic or bioinformatic approaches (37, 38).

Replicating or not, all cells face the challenge of maintaining an energized membrane, ATP, and carbon precursors. The studies reported herein identify a metabolically unique and bioenergetically efficient mechanism of adapting to a potentially broad range of O_2 concentrations. Other microbes and cell types, such as tumor cells and host cells at inflammatory sites, occupy a similarly diverse range of O_2-limited niches. The mechanism described herein may thus pertain to them as well (48).

Materials and Methods

***M.tuberculosis* Filter Culture and Metabolite Extraction.** *M. tuberculosis* strains H37Rv, Erdman, *icl* knock-out (ΔICL KO) and the complemented strain (ICL::pICL) were cultured in a biosafety level 3 facility at 37 °C in Middlebrook 7H9 broth (m7H9) or on 7H10 agar (m7H10) (Difco) supplemented with 0.2% acetate (or 0.2% glucose in case of Erdman-based mutant strains), 0.04% Tyloxapol (broth only), 0.5 g/L BSA, and 0.085% NaCl. *M. tuberculosis*-laden filters used for metabolomic profiling were generated as previously described (29, 30) and incubated at 37 °C for 5 d to reach the midlogarithmic phase of growth. *M. tuberculosis*-laden filters were then transferred onto chemically identical medium containing fresh ^{12}C acetate or [U-^{13}C] acetate-m7H10. *M. tuberculosis*-laden filters were metabolically quenched by plunging filters into a mixture of acetonitrile/methanol/H_2O (40:40:20) precooled to −40 °C; metabolites were extracted by mechanical lysis with 0.1 mm Zirconia beads in a Precellys tissue homogenizer for 3 min (6,500 rpm) twice under continuous cooling at or below 2 °C. Lysates were clarified by centrifugation and then filtered across a 0.22-μm filter. Residual protein content of metabolite extracts (BCA Protein Assay kit; Thermo Scientific) was determined to normalize samples to cell biomass. 3NP and nitrate (Sigma) were used at 200 μM and 5 mM final concentration, respectively. Extracellular succinate used to inhibit succinate secretion was provided at 2 mM. All data obtained by metabolomics were average of independent triplicates.

In Vitro Hypoxia. In vitro hypoxia was achieved using the type A Bio-bag environmental chamber (Becton Dickinson) as instructed by the manufacturer's instructions and validated by a resazurin indicator, which decolorized at oxygen concentrations of 1.0% or less. *M. tuberculosis*-laden filters were transferred to fresh chemically equivalent m7H10 agar medium immediately before insertion or after recovery from sealed hypoxic chambers. *M. tuberculosis*-laden filters recovered from hypoxic chambers were immediately plunged into the precooled quenching solution as described above.

Metabolomics with Liquid Chromatography-Mass Spectrometry. LC-MS–based metabolomics analysis was used to report alternate metabolic state of hypoxia-induced nonreplicating *M. tuberculosis*. Extracted metabolites were separated on a Cogent Diamond Hydride type C column (gradient 3) (49). The mobile phase consisted of the following: solvent A (ddH_2O with 0.2% formic acid) and solvent B (acetonitrile with 0.2% formic acid). The gradient used was as follows: 0–2 min, 85% B; 3–5 min, 80% B; 6–7 min, 75%; 8–9 min, 70% B; 10–11.1 min, 50% B; 11.1–14 min 20% B; 14.1–24 min 5% B followed by a 10 min reequilibration period at 85% B at a flow rate of 0.4 mL/min. The mass spectrometer used was an Agilent Accurate Mass 6220 time of flight (TOF) coupled to an Agilent 1200 liquid chromatography (LC) system. Dynamic mass axis calibration was achieved by continuous infusion of a reference mass solution using an isocratic pump with a 100:1 splitter. This configuration achieved mass errors of 5 ppm, mass resolution ranging from 10,000 to 25,000 (over *m/z* 121–955 atomic mass units), and 5 $\log_{10}$ dynamic range. Detected ions were deemed metabolites on the basis of unique accurate mass-retention time identifiers for masses exhibiting the expected distribution of accompanying isotopomers. Metabolite identities were searched for using a mass tolerance of <0.005 Da. Metabolites were quantified using a calibration curve generated with chemical standard spiked into homologous mycobacterial extract to correct for matrix-associated ion suppression effects.

Isotopomer Data Analysis Using Isotope-Labeled Carbon Sources. The extent of isotopic labeling for metabolites was determined by dividing the summed peak height ion intensities of all labeled isotopologue species by the ion intensity of both labeled and unlabeled species, expressed in percentage. Label-specific ion counts were corrected for naturally occurring ^{13}C species (i.e., [M+1] and [M+2]). The relative abundance of each isotopically labeled species was determined by dividing the peak height ion intensity of each isotopic form (corrected for naturally occurring ^{13}C species as above) by the summed peak height ion intensity of all labeled species. Ion intensities were converted into molar abundances using standard curves generated by addition of chemical standards and serial dilution of samples to establish the colinearity of ion intensity and molar abundance.

Cell Viability Test. *M. tuberculosis* viability was determined using liquid cultures manipulated under experimentally identical conditions as filter-grown cultures used for metabolomic profiling, which we had previously demonstrated to be microbiologically similar. CFUs were determined by plating on m7H11 agar with supplements; 0.2% glycerol, 0.2% glucose, 0.5 g/L BSA, and 0.085% NaCl. CFUs for Erdman WT, ΔICL KO, and ICL::pICL strains were measured by using m7H9 with Bacto agar due to the apparent toxicity of malachite green to ΔICL KO.

Extraction of RNA and Quantitative Real-Time PCR. Total RNA was extracted from *M. tuberculosis*-laden filters (cultured similarly to samples used for metabolomic profiling) (28). *M. tuberculosis* cells were resuspended in 1 mL cold TRIzol (Gibco/BRL) and transferred to 2 mL screw-cap tubes containing 0.4 mL of 0.1 mm diameter Zirconia/silica beads (BioSpec Products). Cells were disrupted by 30-s pulses in a BioSpec Products bead beater three times. Lysates were then centrifuged at 13,000 × *g* for 10 min at 4 °C and supernatants were subsequently transferred to fresh tubes. The supernatant was then transferred to a tube containing 200 μL chloroform, inverted for 1 min, and centrifuged at maximum speed. The aqueous phase was then precipitated using 500 μL 80% ethanol. RNA was isolated using an RNeasy kit following manufacturer's recommendations (Qiagen). The concentrations of extracted purified total RNA (wt/vol) were measured using a Nanodrop spectrophotometer. qRT-PCR was performed in 20-μL volumes using the iScript one-step RT-PCR kit with Sybr green (Bio-Rad Laboratories) on a LightCycler 480 Real-Time PCR System (Roche). Reactions were set up as per the manufacturer's instructions, using 100 ng of total RNA. The amplification procedure was as follows: cDNA synthesis for 30 min at 50 °C; RT inactivation for 5 min at 95 °C; and PCR cycling and detection (40 cycles) for 30 s at 95 °C, 30 s at annealing temperature (60 °C), and 30 s at 76 °C (acquiring signal at the end of this step). For all reactions, several no-RT and no-template controls were carried out and yielded no detectable signals. The primers used here are as follows: *dosR*-F, gacgaccagctgatggtaaaggtcttcttggtcg and *dosR*-R, gaggagggtacctcatggtccatcaccgggtg; *icl*-F, ccaagttccagaaggagctg and *icl*-R, ttcctgcagttcgacatacg; *sigA*-F, cctacgctacgtggtggatt and *sigA*-R, tggatttccagcaccttctc.

Measurement of Intrabacterial ATP Content and NADH/NAD Ratios. *M. tuberculosis*-laden filters as used for metabolomic profiling were separately generated to measure intrabacterial ATP and NADH/NAD content. Intrabacterial ATP concentrations were measured by BacTiter-Glo Microbial Cell Viability Assay according to the manufacturer's instructions (Promega). NAD and NADH concentrations were measured using a FluroNAD/NADH detection kit (Cell Technology). Metabolism of *M. tuberculosis* was rapidly quenching by plunging bacilli in the first solvent in the kit.

Membrane Potential Determination. *M. tuberculosis* membrane potential was measured as previously described and adapted to our in vitro hypoxia apparatus (18, 41). Briefly, *M. tuberculosis* cultures were grown in m7H9

medium with 0.2% acetate to midlogarithmic phase and concentrated to an OD_{580} ~1.0 in fresh m7H9. *M. tuberculosis* cultures were then inoculated into 96-well microtiter plates and inserted into the hypoxia chamber already preinstalled with a squeezable, plastic Pasteur pipette loaded with 15 μM $DiOC_2$ affixed to the roof of the chamber as depicted in Fig S2*B*. After 48 h of hypoxic incubation, 15 μM $DiOC_2$ was added to the well and incubated for 20 min at room temperature, followed by fixation with 1% formaldehyde for an additional 10 min (18). Cultures were then subsequently washed with fresh m7H9 to remove extracellular dye. As a positive control for membrane depolarization, cultures grown under ambient air condition were treated with 5 μM of the protonophore carbonyl-cyanide 3-chlorophenylhydrazone (cccp) (Invitrogen). DMSO was used as a vehicle control. The assay was performed in black with clear-bottom 96-well plates (Costar) and a SpectraMax M5 spectrofluorimeter (Molecular Devices) was used to measure green fluorescence (488 nm/530 nm) and shifts to red fluorescence (488 nm/610 nm), as a result of aggregation of dye molecules due to the presence of a large membrane potential. Membrane potential was measured as a ratio of red fluorescence (which depended on cell size and membrane potential) to green fluorescence (which depended on cell size alone). Each condition was measured in triplicate and each experiment was performed twice.

Statistical Analysis. Analyses were performed by the ANOVA test. A *P* value of less than 0.05 was considered statistically significant.

ACKNOWLEDGMENTS. We thank John McKinney for the generous gift of the Erdman and *icl* mutant stains used herein and Carl Nathan, Sabine Ehrt, and Michael Malamy for helpful discussions. This work was supported by National Institutes of Health AI081094, the Bill and Melinda Gates Foundation Grand Challenges Exploration program, and a Burroughs Wellcome Fund Career Award in the Biomedical Sciences (to K.Y.R.), and the Stony Wold Herbert Fund (H.E.). K.Y.R. also received support from the William Randolph Hearst Foundation.

1. Gray JV, et al. (2004) "Sleeping beauty": Quiescence in Saccharomyces cerevisiae. *Microbiol Mol Biol Rev* 68(2):187–206.
2. Bloom BR, Murray CJ (1992) Tuberculosis: Commentary on a reemergent killer. *Science* 257(5073):1055–1064.
3. Barry CE, 3rd, et al. (2009) The spectrum of latent tuberculosis: Rethinking the biology and intervention strategies. *Nat Rev Microbiol* 7(12):845–855.
4. Boshoff HI, Barry CE, 3rd (2005) Tuberculosis: Metabolism and respiration in the absence of growth. *Nat Rev Microbiol* 3(1):70–80.
5. Gill WP, et al. (2009) A replication clock for *Mycobacterium tuberculosis*. *Nat Med* 15(2):211–214.
6. Muñoz-Elías EJ, et al. (2005) Replication dynamics of *Mycobacterium tuberculosis* in chronically infected mice. *Infect Immun* 73(1):546–551.
7. Nathan C, et al. (2008) A philosophy of anti-infectives as a guide in the search for new drugs for tuberculosis. *Tuberculosis (Edinb)* 88(Suppl 1):S25–S33.
8. Lemons JM, et al. (2010) Quiescent fibroblasts exhibit high metabolic activity. *PLoS Biol* 8(10):e1000514.
9. Shi L, et al. (2005) Changes in energy metabolism of *Mycobacterium tuberculosis* in mouse lung and under in vitro conditions affecting aerobic respiration. *Proc Natl Acad Sci USA* 102(43):15629–15634.
10. Shi L, et al. (2010) Carbon flux rerouting during *Mycobacterium tuberculosis* growth arrest. *Mol Microbiol* 78(5):1199–1215.
11. Flynn JL, Chan J (2001) Immunology of tuberculosis. *Annu Rev Immunol* 19:93–129.
12. Russell DG, Barry CE, 3rd, Flynn JL (2010) Tuberculosis: What we don't know can, and does, hurt us. *Science* 328(5980):852–856.
13. Rustad TR, Sherrid AM, Minch KJ, Sherman DR (2009) Hypoxia: A window into *Mycobacterium tuberculosis* latency. *Cell Microbiol* 11(8):1151–1159.
14. Voskuil MI, et al. (2003) Inhibition of respiration by nitric oxide induces a *Mycobacterium tuberculosis* dormancy program. *J Exp Med* 198(5):705–713.
15. Wayne LG, Sohaskey CD (2001) Nonreplicating persistence of *mycobacterium tuberculosis*. *Annu Rev Microbiol* 55:139–163.
16. Warner DF, Mizrahi V (2006) Tuberculosis chemotherapy: The influence of bacillary stress and damage response pathways on drug efficacy. *Clin Microbiol Rev* 19(3): 558–570.
17. Xie Z, Siddiqi N, Rubin EJ (2005) Differential antibiotic susceptibilities of starved *Mycobacterium tuberculosis* isolates. *Antimicrob Agents Chemother* 49(11):4778–4780.
18. Rao SP, Alonso S, Rand L, Dick T, Pethe K (2008) The protonmotive force is required for maintaining ATP homeostasis and viability of hypoxic, nonreplicating *Mycobacterium tuberculosis*. *Proc Natl Acad Sci USA* 105(33):11945–11950.
19. Weinstein EA, et al. (2005) Inhibitors of type II NADH:menaquinone oxidoreductase represent a class of antitubercular drugs. *Proc Natl Acad Sci USA* 102(12):4548–4553.
20. Leistikow RL, et al. (2010) The *Mycobacterium tuberculosis* DosR regulon assists in metabolic homeostasis and enables rapid recovery from nonrespiring dormancy. *J Bacteriol* 192(6):1662–1670.
21. Park HD, et al. (2003) Rv3133c/dosR is a transcription factor that mediates the hypoxic response of *Mycobacterium tuberculosis*. *Mol Microbiol* 48(3):833–843.
22. Voskuil MI, Visconti KC, Schoolnik GK (2004) *Mycobacterium tuberculosis* gene expression during adaptation to stationary phase and low-oxygen dormancy. *Tuberculosis (Edinb)* 84(3-4):218–227.
23. Rustad TR, Harrell MI, Liao R, Sherman DR (2008) The enduring hypoxic response of *Mycobacterium tuberculosis*. *PLoS One* 3(1):e1502.
24. Watanabe S, et al. (2011) Fumarate reductase activity maintains an energized membrane in anaerobic *Mycobacterium tuberculosis*. *PLoS Pathog* 7(10):e1002287.
25. Marrero J, Rhee KY, Schnappinger D, Pethe K, Ehrt S (2010) Gluconeogenic carbon flow of tricarboxylic acid cycle intermediates is critical for *Mycobacterium tuberculosis* to establish and maintain infection. *Proc Natl Acad Sci USA* 107(21):9819–9824.
26. McKinney JD, et al. (2000) Persistence of *Mycobacterium tuberculosis* in macrophages and mice requires the glyoxylate shunt enzyme isocitrate lyase. *Nature* 406(6797): 735–738.
27. Muñoz-Elías EJ, McKinney JD (2005) *Mycobacterium tuberculosis* isocitrate lyases 1 and 2 are jointly required for *in vivo* growth and virulence. *Nat Med* 11(6):638–644.
28. Schnappinger D, et al. (2003) Transcriptional adaptation of *Mycobacterium tuberculosis* within macrophages: Insights into the phagosomal environment. *J Exp Med* 198(5):693–704.
29. Brauer MJ, et al. (2006) Conservation of the metabolomic response to starvation across two divergent microbes. *Proc Natl Acad Sci USA* 103(51):19302–19307.
30. de Carvalho LP, et al. (2010) Metabolomics of Mycobacterium tuberculosis reveals compartmentalized co-catabolism of carbon substrates. *Chem Biol* 17(10):1122–1131.
31. Aly S, et al. (2006) Oxygen status of lung granulomas in *Mycobacterium tuberculosis*-infected mice. *J Pathol* 210(3):298–305.
32. Heng Y, et al. (2011) *Mycobacterium tuberculosis* infection induces hypoxic lung lesions in the rat. *Tuberculosis (Edinb)* 91(4):339–341.
33. Via LE, et al. (2008) Tuberculous granulomas are hypoxic in guinea pigs, rabbits, and nonhuman primates. *Infect Immun* 76(6):2333–2340.
34. Blumenthal A, Trujillo C, Ehrt S, Schnappinger D (2010) Simultaneous analysis of multiple *Mycobacterium tuberculosis* knockdown mutants *in vitro* and *in vivo*. *PLoS ONE* 5(12):e15667.
35. Ehrt S, Schnappinger D (2009) Mycobacterial survival strategies in the phagosome: Defence against host stresses. *Cell Microbiol* 11(8):1170–1178.
36. Sherman DR, et al. (2001) Regulation of the *Mycobacterium tuberculosis* hypoxic response gene encoding alpha -crystallin. *Proc Natl Acad Sci USA* 98(13):7534–7539.
37. Beste DJ, et al. (2011) ^{13}C metabolic flux analysis identifies an unusual route for pyruvate dissimilation in mycobacteria which requires isocitrate lyase and carbon dioxide fixation. *PLoS Pathog* 7(7):e1002091.
38. Wayne LG, Lin KY (1982) Glyoxylate metabolism and adaptation of *Mycobacterium tuberculosis* to survival under anaerobic conditions. *Infect Immun* 37(3):1042–1049.
39. Timm J, et al. (2003) Differential expression of iron-, carbon-, and oxygen-responsive mycobacterial genes in the lungs of chronically infected mice and tuberculosis patients. *Proc Natl Acad Sci USA* 100(24):14321–14326.
40. Engel P, Krämer R, Unden G (1994) Transport of C4-dicarboxylates by anaerobically grown *Escherichia coli*. Energetics and mechanism of exchange, uptake and efflux. *Eur J Biochem* 222(2):605–614.
41. de Carvalho LP, Darby CM, Rhee KY, Nathan C (2011) Nitazoxanide disrupts membrane potential and intrabacterial pH homeostasis of *Mycobacterium tuberculosis*. *ACS Med Chem Lett* 2(11):849–854.
42. Alston TA, Mela L, Bright HJ (1977) 3-Nitropropionate, the toxic substance of Indigofera, is a suicide inactivator of succinate dehydrogenase. *Proc Natl Acad Sci USA* 74(9):3767–3771.
43. Rhee KY, Erdjument-Bromage H, Tempst P, Nathan CF (2005) S-nitroso proteome of *Mycobacterium tuberculosis*: Enzymes of intermediary metabolism and antioxidant defense. *Proc Natl Acad Sci USA* 102(2):467–472.
44. Sohaskey CD (2008) Nitrate enhances the survival of *Mycobacterium tuberculosis* during inhibition of respiration. *J Bacteriol* 190(8):2981–2986.
45. Tan MP, et al. (2010) Nitrate respiration protects hypoxic *Mycobacterium tuberculosis* against acid- and reactive nitrogen species stresses. *PLoS ONE* 5(10):e13356.
46. Sohaskey CD, Wayne LG (2003) Role of *narK2X* and *narGHJI* in hypoxic upregulation of nitrate reduction by *Mycobacterium tuberculosis*. *J Bacteriol* 185(24):7247–7256.
47. Nathan C (2009) Taming tuberculosis: A challenge for science and society. *Cell Host Microbe* 5(3):220–224.
48. Vander Heiden MG, Cantley LC, Thompson CB (2009) Understanding the Warburg effect: The metabolic requirements of cell proliferation. *Science* 324(5930):1029–1033.
49. Pesek JJ, Matyska MT, Fischer SM, Sana TR (2008) Analysis of hydrophilic metabolites by high-performance liquid chromatography-mass spectrometry using a silica hydride-based stationary phase. *J Chromatogr A* 1204(1):48–55.